Available online at www.sciencedirect.com
ScienceDirect
BioSystems 88 (2007) 228–242
BioSystems
www.elsevier.com/locate/biosystems

Brownian motion, fluctuation and life

Toshio Yanagida [a,b,*], Masahiro Ueda [a], Tsutomu Murata [c], Seiji Esaki [a], Yoshiharu Ishii [b]

[a] *Graduate School of Frontier Biosciences, Osaka University, 1-3 Yamadaoka, Suita, Osaka 565-0871, Japan*
[b] *Formation of Soft Nano-machines, CREST, 1-3 Yamadaoka, Suita, Osaka 565-0871, Japan*
[c] *Kobe Advanced ICT Research Center, Brain Information Project, Iwaoka, Nishi-ku, Kobe, Hyogo 651-2492, Japan*

Received 26 June 2006; accepted 25 August 2006

Abstract

The measurements of dynamic behaviors of biomolecules in relation to their functions have been allowed using single molecule measurements. Thermal Brownian motion causes random step motion of motor proteins and structural fluctuation of protein molecules between multiple states. In hierarchic structure of life, the fluctuation is modulated. Random fluctuation is biased to directional motion and reactions as a result of interaction of proteins. The fluctuation of kinetic state of signaling proteins results in polarization and localization of cells. A recognition process in brain is also explained by the equation analogous to biochemical reaction at the molecular level. Thus dynamic processes originated from thermal motion may play an important role in activation processes in life.

Keywords: Fluctuation, Brownian motion, Single molecule measurement, Molecular motor, Cell signaling process, Dynamic structure of protein, Recognition in brain

Fluctuations are ubiquitous in various stages from molecules to brains in life science (Fig. 1). Fluctuations are only noises in some cases. It has been demonstrated that fluctuations are fundamental to the function of biological systems. Random thermal motion is the origin of fluctuation. Motion and energy fluctuations are not randomized in a short time period on the scale of biomolecules. The thermal motion is modulated, when atoms and molecules are fabricated into large biomolecules, molecular machines and varieties of biosystems. At the same time fast thermal motion stimulates collective motion of whole biomolecules to occasionally change physical and chemical states in slow time scale. These transition changes occur when fluctuating energy of molecules exceeds a threshold. The result is not uniquely determined but is stochastic. Several results are possible with some probability, in contrast to a mechanical system in which the result is deterministic. In ensemble measurements, the obtained values which are average values over many molecules have been interpreted as deterministic values. However, in biological systems, the average values are not necessarily effective, but the values of individual molecules play a role. In many cases (simplest cases) one of two states, A or B appears. Between two states the system spontaneously fluctuates and one of the two states occurs alternately (Scheme 1).

* Corresponding author. Tel.: +81 6 6879 4630; fax: +81 6 6879 4634.
E-mail addresses: yanagida@phys1.med.osaka-u.ac.jp (T. Yanagida), ueda@phys1.med.osaka-u.ac.jp (M. Ueda), benmura@po.nict.go.jp (T. Murata), esaki@phys1.med.osaka-u.ac.jp (S. Esaki), ishii@phys1.med.osaka-u.ac.jp (Y. Ishii).
URL: http://www.phys1.med.osaka-u.ac.jp/ (T. Yanagida).

0303-2647/$ – see front matter © 2006 Elsevier Ireland Ltd. All rights reserved.
doi:10.1016/j.biosystems.2006.08.012

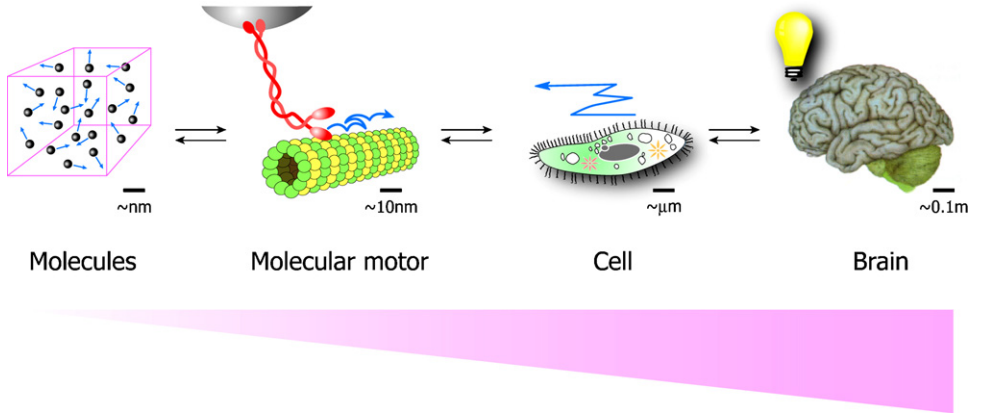

Fig. 1. Hierarchic structure of biological structures. Thermal motion in different stages of hierarchic structures of biological systems.

$$A \rightleftarrows B$$

Scheme 1.

Or one of two arises, A or B, following a cycle of reactions (Scheme 2).

For example, molecular motors move forward or backward (A or B) when they undergo the reaction of ATP hydrolysis (represented by a circle).

When fluctuating biomolecules interact with other molecules in biological systems, A or B is preferentially selected and the systems are activated or deactivated. Thermally driven step movement of molecular motors is biased in one direction as a result of the interaction of motor and track proteins. Preferential binding of ligands to one of the spontaneously fluctuating structures of proteins leads to activation or deactivation. Cooperativity, heterogeneity and asymmetry of the activation or deactivation processes are brought about, while the biomolecules are arranged spatially and temporary. This mechanism may be essential for a system in which molecules self-assemble, self-organize or self-control. Recently the thermal fluctuation processes have been directly revealed using single molecule measurements and the mechanism involving fluctuation has been discussed based on these findings.

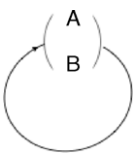

Scheme 2.

1. Measurements of fluctuation at the single molecule level

The observation of Brownian movement of pollen grains in the nineteenth century led to the idea of thermal motion of molecules and the kinetic theory. From this observation the existence of molecules was inferred and the kinetic theory of molecules was built to calculate the average values which can be compared with the values measured in ensemble measurements. Recently developed single molecule measurements allowed dynamic behavior of individual molecules to be measured in real time and the Brownian movement of working biomolecules to be measured directly. Brownian motion is now a research target not only in physics and chemistry but also in life science.

Single molecule techniques consist of imaging and manipulation (Ishijima and Yanagida, 2001; Ishii et al., 2001). The imaging techniques allow behavior of biomolecules such as movement, chemical reaction, structural changes and interactions of single molecules to be visualized. Manipulation techniques allow the interaction of biomolecules to be studied in a controlled manner at the single molecule level and mechanical properties of single biomolecules to be measured. Biomolecules are nanometers in size, too small to be visualized under a light microscope. To visualize them, large probes such as a bead, microneedle or bright probes like small fluorescent molecules are attached and monitored as markers of the biomolecules.

By monitoring changes in position of probes fixed to the biomolecules, displacement of the biomolecules can be measured (Fig. 2) (Finer et al., 1994; Ishijima et al., 1994; Kitamura et al., 1999; Svoboda et al., 1993). Even though the images of the probes are large (~μm),

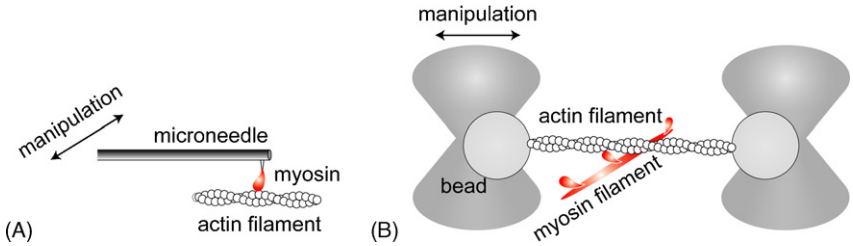

Fig. 2. Manipulation of molecular motors and force measurements. (A) Manipulation of a single myosin molecule with a microneedle. A myosin molecule captured at a tip of the microneedle is allowed to interact with an actin filament placed on a glass surface. (B) Manipulation of an actin filament by a laser trap. Two beads attached at both ends of an actin filament are trapped by laser. The actin filament is manipulated to interact with myosin molecules on the filament placed on a glass surface. In both cases, the movement takes place against the bending and trapping force. The relative movement between actin and myosin is measured by displacement of the microneedle or beads trapped by laser. The microneedle or beads undergoes thermal motion and the strong interaction between myosin and actin reduces the thermal motion.

changes in position can be determined with nanometer accuracy. For example, the image of a bead or a microneedle are projected onto a pair of photodiode and the small changes in the position (even in the order of nm) can be measured from changes in intensity recorded by the two photodiodes. The large probes such as beads and microneedles are also used for manipulation of single molecules. Using the manipulation tools, biomolecules are caused to interact with other molecules at desired positions. This allows us to monitor the single molecule reaction in a controlled manner. The large probes are also used for the mechanical measurement of single molecules. When the single molecules attached to the large probes are pulled, a trapping force or bending force is exerted on the biomolecules against the pulling force. When molecular motors attached to large probes move actively, the exerted force act against the movement. Thus, it is possible to measure the mechanical properties of the single molecules under the external force. For accurate measurements, the thermal fluctuation of the position of a bead or microneedle must be reduced. The mean square displacement $\langle x^2 \rangle$ of a bead and microneedle is related to the stiffness of the measurement system by an equipartition law such as $K\langle x^2 \rangle/2 = k_B T/2$. The root mean square distance decreases as a spring constant increases or the system becomes stiff.

Fluorescent probes are used for fluorescence imaging. Single molecules are visualized as fluorescent spots when the molecules stay at the same position (Funatsu et al., 1995). When fluorescence probes are excited by a laser, fluorescence is detected at a different color from the color of the excitation laser, so we can monitor them distinguishably from other molecules even in the scene where varieties of biomolecules coexist. The motion of the molecules is measured by tracing the fluorescent spots. However, the fluorescent spot from a biomolecule 1 nm in size is expanded to ~100 nm inevitably due to the diffraction limit of light. The fluorescence intensity distributes in Gaussian distribution function around a real position of the molecule. The position of the molecule can be measured by experimentally determining the Gaussian distribution function with about 10 nm accuracy. To monitor the structural changes of biomolecules, fluorescence spectroscopy techniques are combined with single molecule imaging. For example, fluorescence resonance energy transfer (FRET) is a technique to measure the distance in a 2–10 nm range (Lakowicdz, 1999). Single molecule FRET has been used for measurements of the dynamics of protein interactions and structures (Weiss, 1999).

The measurements of fluorescence involve counting photons emitted from single fluorohore (Fig. 3). Fluorescence intensity is a measurement of the number of photons acquired in a constant time period. In fluorescence techniques such as fluorescence spectrum, fluorescence polarization, FRET and position detection, numbers of photons are counted as a function of parameters such as wavelength, polarization direction and pixel positions. The parameter-dependent fluorescence intensity profile gives information on the biomolecules to which the probes are attached. In the measurements, photon detection occurs randomly due to the stochastic nature of photochemical reactions. The number of photons ends up fluctuating. The resolution of the determination of the fluorescence profiles depends on the number of photons; as the number of photons increases, the parameter-dependent profiles such as Gaussian distribution function for position determination are measured more accurately and better results are obtained. However, larger numbers of photons requires longer acquisition time with sacrifice of time resolution.

The stochastic nature of the detection of photons in fluorescence measurements and the compliance of the connections between the large probes and biomiolecules

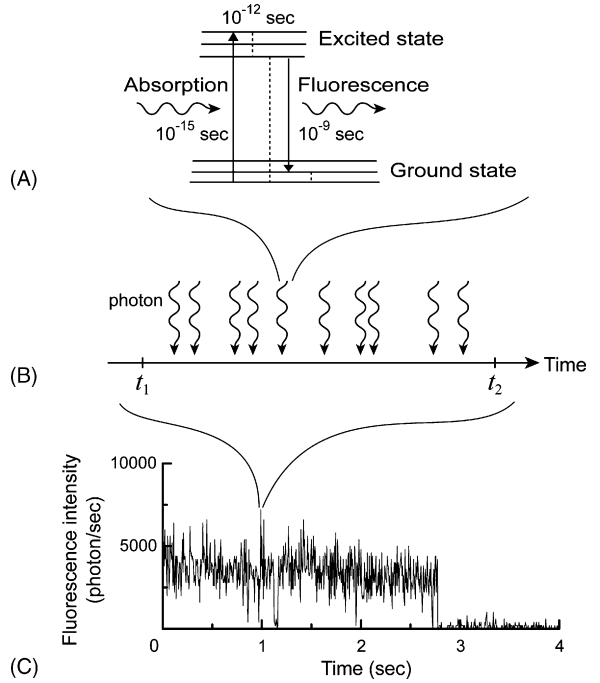

Fig. 3. Photon-counting and fluorescence measurements. (A) Mechanism for fluorescence emission. Photons are emitted after series of photochemical reactions of electronic states of fluorescent molecules in the timescale of nanoseconds. (B) Photon emission from a single fluorescent molecule occurs randomly. (C) Fluorescence measurements are performed by counting the number of photon emitted from a single molecule detected in a period of time (ms–s). Reflecting the stochastic nature of the photon detection, the fluorescence intensity fluctuates.

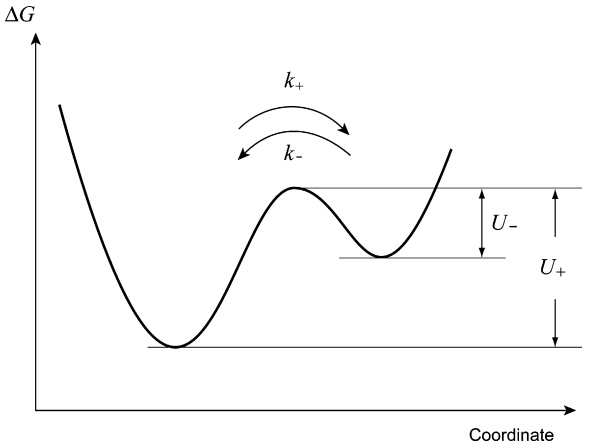

Fig. 4. Energy landscape for dynamics of biomolecules. Energy landscape is described as free energy of biomolecules as a function of their coordinates such as positions and structural parameters. At local minima, biomolecules are stable and fluctuate around the minima. When biomolecules change from one local minimum to the other through an activation energy barrier, the rate, $k_{\pm}$ for forward and backward steps, is represented by the ratio of the activation energy $\Delta U_{\pm}$ to thermal energy $k_{\mathrm{B}}T$ in Arrhenius equilibrium $k_{\pm} \sim \exp[-(\Delta U_{\pm}/k_{\mathrm{B}}T)]$. The free energy of the molecules fluctuates and they undertake a transition when the energy value is greater than the activation energy.

in the mechanical measurements cause fluctuation of the measurements, making accurate measurements difficult. When the signals from biomolecules change in a stochastic manner, we have to design the experiments and analysis to discriminate fluctuations originating from the experimental systems from those generated by the biomolecules. The characteristic time constant is a key to distinguish them.

For the events that occur in a stochastic manner, the measurement of single events does not solely characterize the system. The value obtained by a single event is only one of the possible numbers. One needs to repeat the measurement many times and analyze the data statistically. The average values are consistent with the data from ensemble measurements and the time sequence and distribution are useful information that single molecule measurements provide uniquely. The basic equation used for the kinetic analysis is originally defined as change in the concentrations for ensemble measurements. In single molecule measurements, the same equation has been used as the concentrations is read as probabilities. The thermal processes are described using thermodynamic parameters and the energy landscape of biomolecules (Fig. 4).

2. Forward or backward step movement of kinesin

Molecular motors are responsible for motile activities including muscle contraction, cell morphology, and vesicle transport (Schliwa, 2003). Basis of these motile activities at molecular level is relative movement between a pair of protein molecules, motor and linear protein tracks. Active movement by molecular motors is distinguished from diffusion movement by directionality; in diffusion movement the direction of movement changes randomly while active movement is directed in one direction. The energy required for directional movement is released from breakdown of ATP to ADP, which occurs in a stochastic manner.

Kinesin is a molecular motor ∼10 nm in size, that transports vesicles along a protein track called microtubules in cells (Fig. 5A). Kinesin moves using two head domains (motor domains including ATP and microtubule binding sites) connected at the tail domain. At the motor domain kinesin hydrolyzes ATP and interacts with microtubules. The two heads alternately step on the binding sites arranged regularly in an 8-nm interval on microtubules (hand-over-hand mechanism) (Fig. 5B) (Nishiyama et al., 2002; Taniguchi et al., 2005). Starting

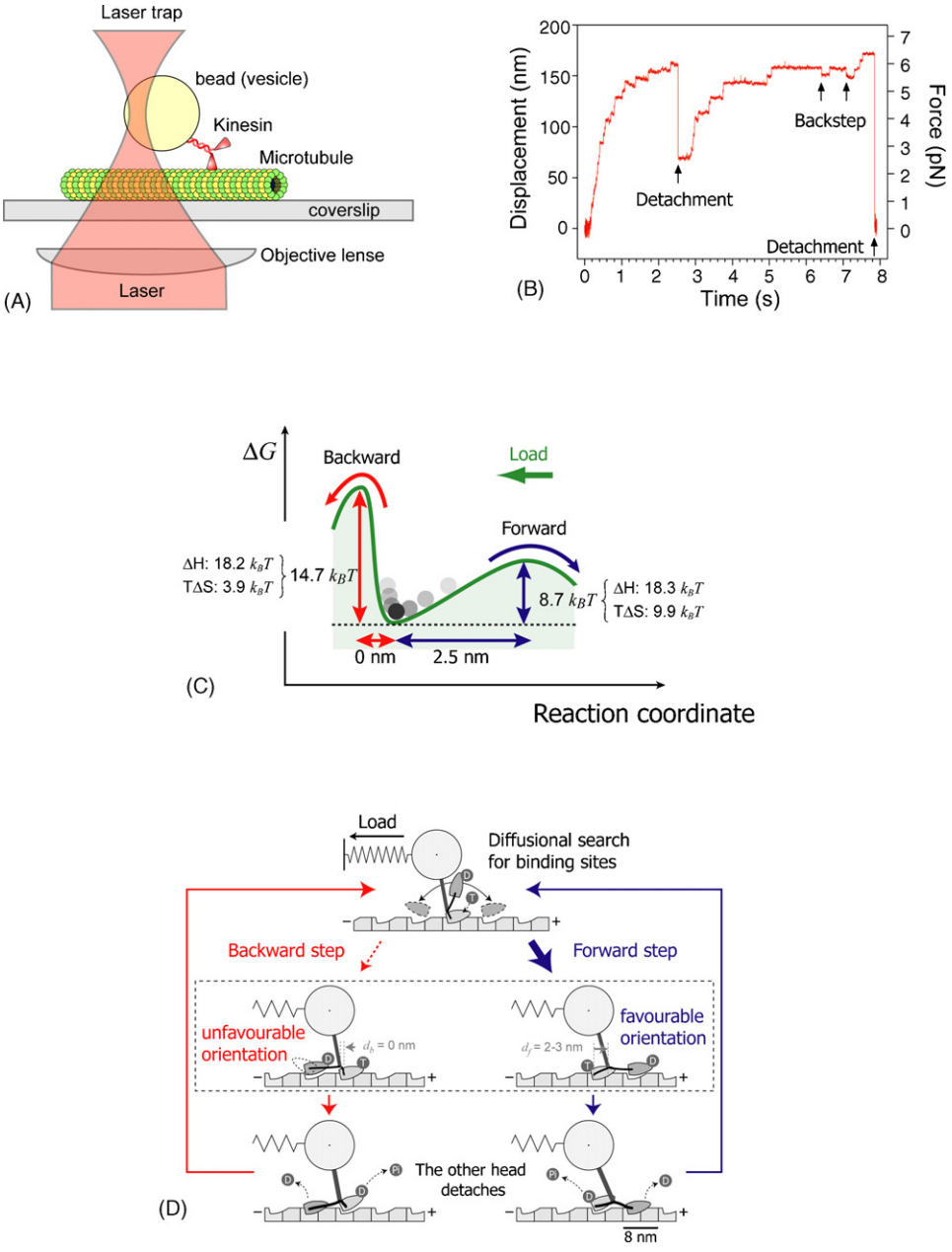

Fig. 5. Forward and backward step movement of kinesin. (A) A single kinesin molecule moving on microtubules. A kinesin molecule is attached to a bead trapped by a focused laser as a cargo for measurements. (B) Time trajectory of displacement and force of kinesin. In the laser trap measurement, when kinesin moves the trapping force or external load increases indicted. (C) Energy landscape for the forward and backward step of kinesin. The thermodynamic parameters obtained for the forward and backward step movement of kinesin are included in the figure. The rates for the forward and backward steps, $k_{\pm}$, are related to the activation energy $U_{\pm}$ and external load F, $k_{\pm} = \text{constant} \exp[-(U_{\pm} + Fd_{\pm})/k_B T]$ where $d_{\pm}$ is a characteristic distance and $\pm$ denotes forward and backward steps. $U_{\pm}$ was break down to enthalpic contribution $H_{\pm}$ and entropic contribution $S_{\pm}$, $U_{\pm} = H_{\pm} - TS_{\pm}$. The difference in the activation energy is mainly explained by the difference in entropy. (D) A model for preferential binding of kinesin to one direction based on the experimental results summarized in (C).

from the state that one head is attached to a binding site on microtubules and the other is detached, the detached head diffuses back and forth searching for the next binding sites on microtubules. The detached head attaches to a neighboring binding site in either forward or backward directions, followed by the detachment of the other head to complete one cycle of the step movement. If the detached head attaches to the forward position, this step

is a forward step. If the detached head is attached to the backward position, this step is a backward step.

Attachment to and detachment from microtubules is coupled to the ATP hydrolysis reaction. Kinesin attaches to microtubules when bound ATP is hydrolyzed and detaches when the products of the ATP hydrolysis is released. The time intervals between the step movement vary, reflecting the stochastic nature of the ATP hydrolysis reactions. In simplest case, the reaction is described as a sequence of binding of ATP, ATP hydrolysis and release of the products, ADP and Pi in a Michaelis-Menten form. Average timing is dependent on the parameters such as the ATP concentration, load and temperature. The ATP binding steps depend on the probability that kinesin molecules encounter ATP molecules in solution. The stepwise movement of kinesin has been measured by monitoring the displacement of beads attached to single kinesin molecules, which move along microtubules immobilized on the glass surface. The interval time between step movement was measured as a function of the ATP concentration, load and temperature (Nishiyama et al., 2002; Taniguchi et al., 2005). The distributions and mean values of the interval time were used for analysis of the mechanochemical reactions underlying step movement. In the case of kinesin, the processes were composed of force-independent chemical steps and force-dependent mechanical step (Scheme 3).

As a result of diffusional search, the step movement occurs either in the forward or backward direction. In the absence of external load, however, the step movement occurs overwhelmingly in one direction. The chance to find the backward steps is only 1 step out of 2000 steps. As external load increases, the frequency of the backward step increases relative to the forward step and successive 8-nm backward steps are observed in the presence of excessive load. Thus, both forward and backward steps take place and one of the directions is favored depending on the load. The bias of the directionality is attributable to preferential attachment of the head after diffusional search. In the energy landscape of forward and backward step movement, the directional movement is described as a lower activation free energy barrier for the forward step as compared with the backward step (Fig. 5C). The difference in the activation free energy between the forward and backward movement, which determine the directionality, was $\sim 6k_BT$. From structural studies it has been suggested that the conformational docking at a short region called the neck linker, which is located between the head and coiled-coil tail domain, biases the step movement of the other head toward the forward position. However, the energy reported for the docking ($1–2k_BT$) is not sufficient to explain the difference in the free energy barrier between forward and backward directions.

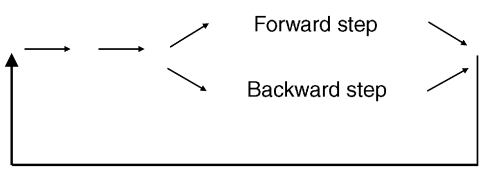

Scheme 3.

The activation free energy U was break down to enthalpic contribution H and entropic contribution S, as $U = H - TS$. The temperature dependence of the step movement of kinesin showed that the difference in the activation free energy between the forward and backward movement is mainly entropic rather than enthalpic (Taniguchi et al., 2005). What is the entropy difference in the binding between the forward and backward direction? One possibility is sterically restricted geometry between the kinesin head and the binding sites on microtubules (Fig. 5D). The kinesin head orients in the opposite direction relative to the orientation of the microtubule when it is located in the forward or backward positions. In the forward position, the most favorable orientation of the kinesin head coincides with the orientation of the binding site on microtubules. In contrast, the favorable orientation of the kinesin head is incompatible to the orientation of the binding site on microtubules in the backward position. Thus, the preferential binding to the forward sites can be explained by geometrical asymmetry of the orientation of the kinesin head and the kinesin binding site on microtubules.

In the free energy landscape it is interpreted that in the presence of external load kinesin moves against external force for a distance corresponding to a characteristic distance. Asymmetry of the characteristic distance between the forward and backward steps indicates the load-dependent directionality. The increase in the external load raises the energy barrier for the forward step and hardly changes that for the backward step, reflecting the respective characteristic distance.

3. Diffusion-anchored step movement of single-headed myosin

Another example of forward and backward movement during a cycle of ATP hydrolysis is step movement of single-headed myosin. Myosin is a molecular motor that moves along an actin filament. Among various types of myosin, myosin V moves processively like kinesin and has been studied extensively. As kinesin, two-headed myosin V move in a hand-over-hand manner (Mehta et

al., 1999). One head steps while the other head stays bound to the actin filament. The stepsize of myosin V is large, 36 nm. The large stepsize has been widely believed to occur by the rotation of a long and stiff neck domain, which is located between the head and tail domains.

Two-headed myosin VI is also a processive motor with a large stepsize (Rock et al., 2001; Nishikawa et al., 2002). However, the neck domain of myosin VI is too short to explain large step, suggesting the diffusion mechanism. Furthermore, it has been reported that wild-type myosin VI has only one head when it transports vesicles in cells. Generally, single-headed motors must readily dissociate and diffuse away when it steps. In the case of single-headed kinesin, additional interaction with microtubules prevents kinesin from dissociating. In the case of myosin VI, in fact, single-headed myosin VI did not move processively shown by fluorescence imaging (Fig. 6A) (Iwaki et al., 2006). However, when it was attached to 200 nm polystyrene beads as cargoes, single-headed myosin VI moved processively with a large step of 40 nm (Fig. 6B). Thus, the cargoes make the movement of single-headed myosin VI processive.

How do cargoes prevent single-headed myosin VI from dissociating from actin filaments when it steps? The explanation is given by slow diffusion of beads as compared with that of the head. The diffusion constant of the beads 200 μm in diameter is 60-fold lower than the myosin VI head in solution, because the size of the bead is much lager than the myosin VI head. The head of myosin VI is attached at its tail to the bead via flexible 30 nm α-helix connecting the tail and head. When the myosin VI head diffuses rapidly from one binding site to the next site on an actin filament, the bead diffuse slowly, preventing the complex of the myosin VI head and the bead from diffusing away from actin filament. The idea has been supported by experiments showing that the increase in the viscosity enhances the processivity of myosin VI through the decrease in the diffusion constant. In the measurements, the viscosity was decreased by meshwork structure of methylcellulose, which resembles the environment in cells. Thus, diffusion-anchored mechanism makes a large contribution on long-distance transport of vesicles of single-headed myosin VI.

In a cycle of the ATP hydrolysis of myosin VI there are two reaction processes that diffusion is involved in; a process that the bead attached to the actin filament via myosin VI molecule diffuses and a process that the myosin head diffuses from one binding site to the next along actin filaments while the bead almost stays at the same position due to slow diffusion (Fig. 6C). Given

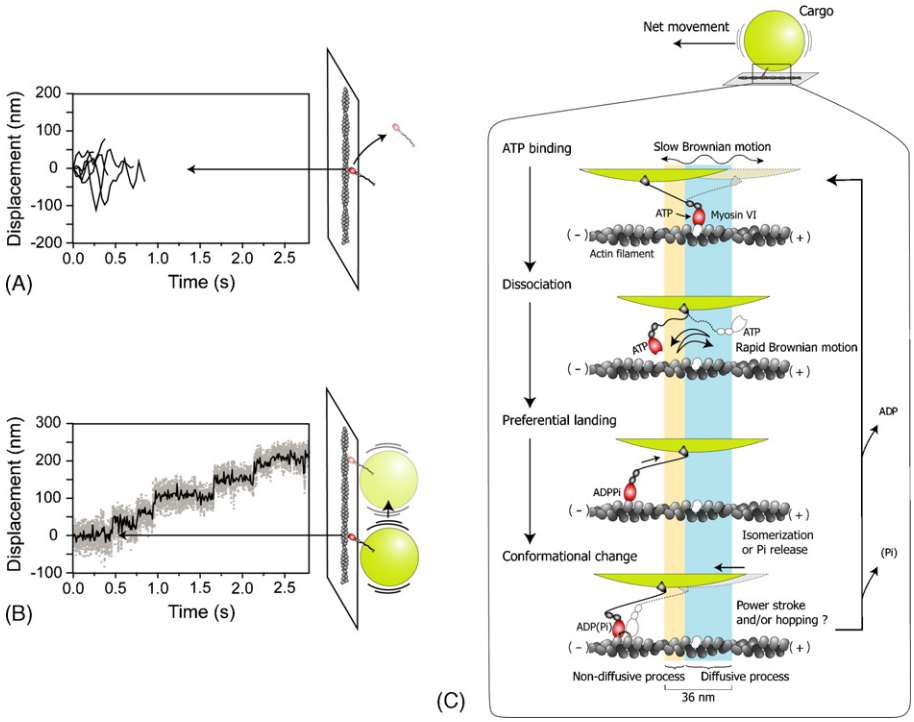

Fig. 6. Diffusion-anchored processive movement of single-headed myosin VI. (A) Non-processive motion of single-headed myosin VI without any cargo. The motion was visualized using green fluorescence protein (GFP) attached. (B) Processive movement of myosin VI with a bead attached as a cargo. (C) Model for diffusion-anchored processive movement of myosin VI.

that although the direction of the movement is opposite to other myosins, myosin VI moves in one direction, the diffusion must be biased to one direction. The preferential binding of the myosin head to the forward direction on the actin filament may cause the bias to directional movement. In the case of myosin VI, we suppose that the myosin head senses the strain applied to it to accelerate the binding of ATP and the release of the products of the ATP hydrolysis. The bead tethered to the actin filament via the myosin VI head diffuse slowly when the head attaches strongly to the actin filament. When the bead diffuses to the forward position, the myosin head is pulled in the forward direction (or the backward strain on the head is relaxed), the binding of ATP to the myosin head is accelerated. The binding of ATP to myosin dissociates the myosin head from actin. When the myosin head diffuses rapidly to the forward position, the myosin head is pulled in the backward position, accelerating the release of Pi. The release of Pi strengthens the binding of the myosin head to actin.

4. Biased Brownian movement of muscle myosin

Multiple steps were found during hydrolysis of single ATP molecules in muscle myosin (myosin II). Unlike myosin V and kinesin, muscle myosin dissociates from actin after every step. In contrast to myosin V and kinesin, where only a small number of molecules participate in carrying cargoes, large number of myosin and actin molecules is organized into a hierarchic structure to generate macroscopic motion and force. Therefore, the time fraction that myosin interacts with actin is low. Only a small number of motor molecules interacting every instant out of large number of motors is sufficient to keep motors on the tracks, even though individual motor molecules are dissociated in most of time. This situation makes it difficult to experimentally track the movement of a single muscle myosin molecule, because it readily diffuses away.

The movement of muscle myosin has been measured by monitoring the changes in the position of either an actin filament interacting with a few myosin molecules immobilized on the glass surface or a single myosin head interacting with actin filaments immobilized on the glass surface. The actin filaments are manipulated by trapping beads attached to the both ends of the filament by a laser. Single myosin molecules are manipulated by attaching them to a tip of a cantilever. Both measurements gave essentially the same results on the movement coupled to the hydrolysis of ATP. When ATP binds to myosin, myosin dissociates from actin and stays at the original position. Then step movement is generated rapidly

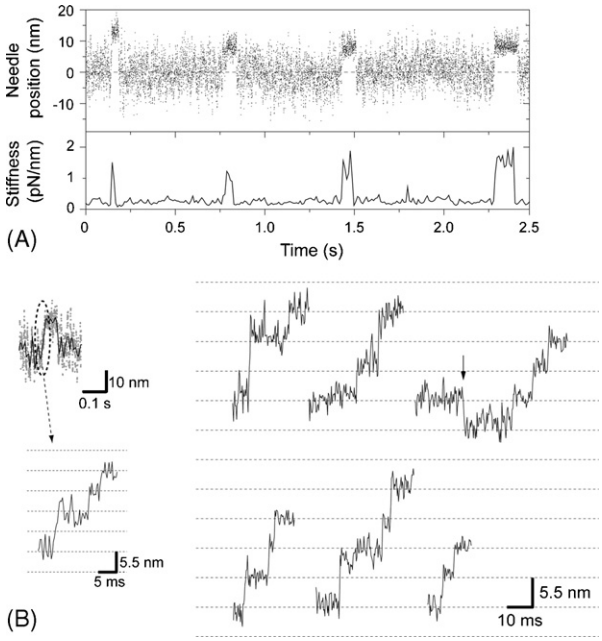

Fig. 7. Biased Brownian movement of myosin II. (A) Non-processive movement of myosin II. (Top) The displacement of the microneedle attached to single myosin II head (S1) was measured as a function of time and the binding of myosin to actin was measured by stiffness calculated from the displacement record (bottom). (B) Expansion of the rising phase of the displacement record above.

and myosin molecules stay displaced until the next ATP molecule binds. This process is repeated continuously.

The steps coupled to the hydrolysis of single ATP molecules have been resolved into multiple stochastic steps using the scanning probe method (Fig. 7) (Kitamura et al., 1999). The laser trap method, however, has not resolved the step so far, probably because of the compliance existing within the measurement systems. The step size of the substeps is 5.5 nm corresponding to the interval of actin monomers. The 5.5 nm step occurs both in the forward and backward direction but overall movement is preferred in one direction. The movement of myosin is interpreted as biased Brownian movement. The energy released from the ATP hydrolysis is most likely used. The ratio of the forward and backward step was 10:1 at no load and decreased with load. The difference in the activation free energy between the forward and backward step was 2–3 k_BT. Several models have been proposed to explain the asymmetric potential. The conformational change in actin filament is one possibility. The other possibility is steric compatibility of the interaction between myosin and the actin filament.

The average total number of the 5.5 nm steps during the hydrolysis of single ATP molecules is 2.5 and the number distributes with the maximum number of 5. The

distribution of the stepsize of the displacement during the hydrolysis of single ATP molecules is interpreted as the distribution of the number of the 5.5 nm steps. There are several possible mechanisms to stop the movement including a strain sensor, conformational changes and chemical reactions of nucleotide. Among them is geometrical restriction due to the protein arrangement in the measurements. The maximum number of the total steps, 5, is within the number of the actin monomer contained in a half pitch of the filament. The myosin heads attached to a scanning probe binds to any of actin monomers in the filament configuration and moves along one of the actin protofilaments down the potential. Changing tracks to the other actin strand is unfavorable, since the myosin head is required to bend and rotate. Finally the step movement of myosin head is blocked by the glass surface. To move further along the filament, myosin heads should change the track to another strand of the filament. Thus, movement of myosin heads is restricted within a half pitch of the filament. When external load is applied, the velocity of the step movement of myosin heads attached to a scanning probe slows down by increasing the interval time of the 5.5 nm steps and by decreasing the number of the 5.5 nm steps, while the stepsize of the 5.5 nm steps is constant. The velocity–force profile is basically the same as that of muscle.

Recently similar results are obtained for single-headed myosin V head constructs with different length of the neck domains. The size of the substeps is constant 5.5 nm. Thus, the 5.5 nm steps occur not only for muscle myosin but also for processive myosin.

Muscle myosin works in a specific and highly ordered array in muscle fibres. How are characteristic properties of isolated myosin molecules modulated in muscle system? What new features do emerge when stochastic motors assemble? The experiments with myosin filament or muscle have suggested that the average distance of the displacement per hydrolysis of single ATP molecules is calculated to be greater than 60 nm. Cooperative action of myosin heads arranged in a myosin filament is likely to explain the enhancement of the distance per ATP molecule. The model has been proposed based on the biased Brownian movement of muscle myosin.

5. Myosin-activated myosin motility via actin conformational change

Actin filaments are a track for the movement of myosin. Biochemically, actin activates the ATP hydrolysis of myosin. Recently it has been shown that the myosin motility is activated through the conformational changes of actin. Single molecule FRET from doubly labeled actin monomer in the filament has revealed that actin has multiple conformations and spontaneously changes the conformation between them with time (Fig. 8) (Kozuka et al., 2006). The multiple conformations are grouped into at least two states, which can be interpreted as the state in which myosin motility is activated and the state in which myosin motility is inhibited. In the presence of myosin, actin favorably takes the conformation in the state, in which the myosin motility is activated (Scheme 4).

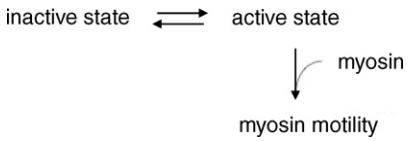

Scheme 4.

The other state is attained when actin is crosslinked chemically. In the crosslinked state, the motility of myosin is inhibited, while the actin-activated ATPase and the binding to actin is not affected. Thus, actin spontaneously fluctuates between the two conformational states that activate and inhibit the myosin motility and the binding of myosin activates the myosin motility by shifting the population of the conformational state of actin.

Multiple conformational states correspond to local minima in the free energy landscape of protein molecules (Fig. 8D). Protein molecules are chains of amino acids that fold in structures in which free energy is locally minimized. Each amino acid has its own physical and chemical properties; some amino acids have positive charges and some negative charges and some have bulky side chains. Free energy of the protein molecules is determined by the sum of all mutual interactions between amino acids on the chain. Minimum positions in the free energy landscape give stable conformations. When thermal motion is allowed, protein molecules dynamically change conformation or move according to landscapes on the free energy landscapes. The structures fluctuate around a stable structure when thermal energy is small or when proteins have only one free energy minimum. As thermal energy increases, protein structures vary between different structures among multiple structures corresponding to multiple local minima in the free energy landscape.

The spontaneous conformational fluctuation of actin is used for various functions when it interacts with its binding proteins. The binding of myosin selects one of the structures to activate its own motility. The self-activation of myosin is mediated through the actin conformation. The activation may become cooperative, when the interaction between actin monomers is rein-

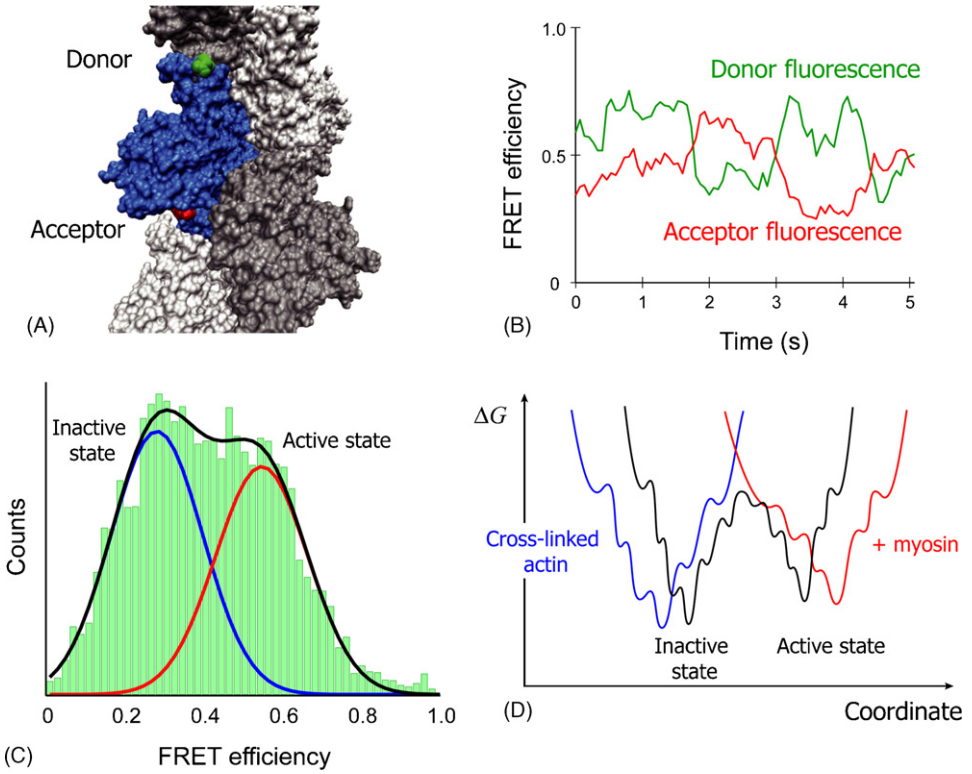

Fig. 8. Spontaneous conformational transition of actin and activation of myosin motility through actin conformational changes. (A) An actin molecule (colored blue) is labeled specifically with donor (green) and acceptor (red) and polymerized with large excess of unlabeled actin (colored grey). (B) Structural dynamics of actin was measured using fluorescence resonance energy transfer (FRET). The time trajectories of the donor (green) and acceptor (red) fluorescence changed due to the changes in FRET; that is, the donor fluorescence increased when the acceptor fluorescence decreased and vice versa. (C) Distribution of the FRET efficiency ($I_A/(I_D + I_A)$ when I_D and I_A are donor and acceptor fluorescence intensity, respectively) from actin. The distribution was fit to two Gaussian distributions corresponding to the high FRET efficiency state or active state in which actin activates the motility of myosin and the low FRET efficiency state or inactive state in which actin inhibits the motility of myosin. (D) Energy landscape of actin. The energy landscape of actin shows two minima corresponding to the active state and inactive state. The energy landscape for actin in the presence of myosin is similar to the active state and that for the cross-linked actin in which myosin motility is inhibited is similar to the inactive state.

forced by other actin binding proteins. Biochemical data showed that in actin alone there is no cooperative activation by the binding of myosin to actin, while in the presence of tropomyosin on the actin filament myosin activates its own binding and ATPase activity in a cooperative manner. Therefore, the conformational change of actin occurs independently in each actin monomer on the filament in the absence of tropomyosin. In contrast, in the complex with tropomyosin, actin conformational changes are transmitted along the filament and the cooperativity along the filament is observed on a macroscopic scale.

Actin plays an important role in cell motility by dynamically forming and deforming actin filaments and their assemblies in collaboration with actin binding proteins. It is intriguing to mention that spontaneous fluctuation of the assembly of actin filaments is the basis of the activation in a similar manner as in dynamic conformational changes of actin molecules found in this study. Actin filaments are self-assembled from actin monomers and the filaments associate and form bundles, networks and gels dynamically in cells. The assembly and disassembly takes place spontaneously and a variety of actin binding proteins are involved in these processes. It has been reported that the activated structure preexists as one of the spontaneously fluctuating structures even in the absence of the external stimuli. The external stimuli do shift the fluctuation towards an activated form. In *Listeria monocytogenes*, an intracellular pathogenic bacterium, in which actin filaments assemble into a polarized alley in response to external stimuli, the polarization has been shown to occur spontaneously through spontaneous assembly of actin even in cell extracts (van Oudenaarden and Theriot, 1999). The basic scheme is analogous to the scheme of the conformational fluctuation, though the conformational role of actin is not known

in dynamic assembly of the actin filaments. Thus, in the case of actin, the structural fluctuation is a key for activation of function on the level of molecules to their higher assemblies.

6. Multiple conformations of Ras and switching signals

Similar conformational fluctuation has been observed for the signaling protein, Ras. Ras, a proto-oncogene product, is a molecular switch in various signaling networks. Cells perform a variety of functions in response to extracellular stimulus such as hormones and neurotransmitters. The signals triggered by the binding of signal molecules to the cell surface are transmitted through signal transduction processes to the nuclei inside the cell. Recently many factors involved in these processes have been identified and several signaling pathways have been elucidated. Ras is a key player in signal transduction processes. When Ras is stimulated, it conforms from an inactivated GDP-bound form to an activated GTP-bound form. Ras in the GTP form can bind to target proteins and activate them. Ras is involved in varieties of signal transduction processes and can interact with various target proteins, triggering respective downstream signaling processes. However, it is not known how Ras recognizes various target proteins to switch signals.

The time trajectory and the histogram of the FRET efficiency showed that in the complex with GTP, Ras has multiple conformational states (Fig. 9A) (Arai et al., 2006). Among them a low FRET inactivated state is distinguished from other high FRET activated states (Fig. 9B). The conformational transition between them occurred in the timescale of seconds. The binding of effectors Ras, Raf or RalGDS, preferentially binds to the activated state and shifts the population of the conformational states from the inactivated state to the activated states. The transition between conformational states within the activated states occurred on the time scale of 20 ms and in the presence of the effectors the transition was not observed, suggesting that Ras stays in

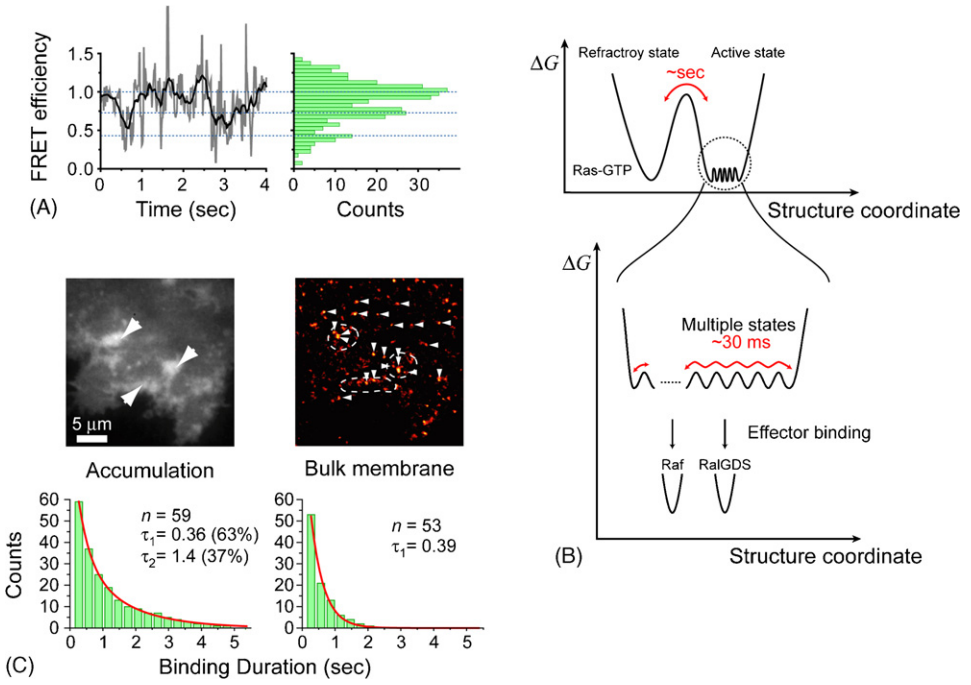

Fig. 9. Multiple conformational and kinetic states of Ras in vitro and in vivo. (A) Conformational dynamics of Ras in vitro. The FRET efficiency changes with time among several FRET efficiency values. Right is the replot of the FRET efficiency in a histogram. (B) Energy landscape model for Ras based on the single molecule measurements of conformational dynamics. *Top*: Refractory state is distinguished from other multiple active states. *Middle*: Among the active states, there are transitions with timescale of ~30 ms. *Bottom*: One of the states is selected upon the binding to effectors. (C) Imaging of the binding of Raf to Ras after stimulation with EGF in living cell cells. Accumulation of fluorescence or GFP labeled Raf was observed (right). After photo bleaching, fluorescence spots (arrows) were observed (right). The binding duration of Raf onto the plasma membrane was measured at accumulation areas (left) and bulk membrane (right). The distribution of the duration time was fit to one or two exponential curves and the decay times determined are indicated.

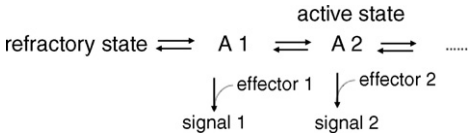

Scheme 5.

one conformational state. Thus, the binding of specific effecters may select a corresponding conformational state out of the multiple conformational states preexisting before binding. Thus, the multiple conformation of Ras may be closely related to the fact that this protein can interact with varieties of target proteins to fulfill corresponding functions (Ito et al., 1997) (Scheme 5).

In living cells, multiple states of Ras were observed in the kinetics of the activation processes. The activation of Ras stimulated by the binding of epidermal growth factor (EGF) to the membrane was visualized by monitoring the recruitment of fluorescently labeled Raf1 that binds to Ras on the plasma membrane in response to activation (Fig. 9C and D) (Hibino et al., 2003). There were at least two kinds of binding sites for Raf1 to the plasma membrane; faster- (0.4 s) and slower- (1.6 s) dissociation sites. The distribution of the kinetic state of Ras was not homogeneous but localized. Raf1 binds to the faster-dissociation site on the bulk membrane, while it binds to both the faster- and slower-dissociation sites on membrane ruffle regions. That is, the slower-dissociation sites are localized specifically at the membrane ruffle regions where cells form active protrusions for migration. These results suggest that Ras has multiple states for Raf1 binding and one specific state is selected at membrane ruffle regions. Multiple conformations of Ras may be a molecular basis for such a heterogeneous activation in living cells.

7. Kinetic heterogeneity of cell signaling processes in living cells

Heterogeneity in kinetic states of signaling molecules was also found in ligand binding reactions to the receptor in chemotaxing *Dictyostelium* cells (Ueda et al., 2001). *Dictyostelium* cells exhibit chemotaxis to chemical gradient of cyclic adenosine 3′,5′-monophosphate (cAMP). *Dictyostelium* cells move randomly in the absence of the gradient of the cAMP concentration and in its presence the movement is preferentially directed in the direction along the gradient of the cAMP concentration. The directional response has been found in various biological processes, including immunity, neuronal patterning, morphogenesis and nutrient finding. To elucidate how cells sense the gradient, we have prepared a fluorescent labeled cAMP (Cy3-cAMP) and visualized the binding to the receptor at the single molecule level in the living cells (Fig. 10). Statistical analysis of lifetimes of Cy3-cAMP bound to the receptor showed that the dissociation rates of Cy3-cAMP were dependent on the pseudopod and tail regions of chemotaxing cells. Cy3-cAMP dissociated faster from the pseudopod regions of the cells than from the tail by a factor of approximately 3. That is, the ligand binding properties of the receptors were not uniform but sensitive to the external chemical gradient in living cells, although the receptor itself distributes uniformly. The differences in the receptor states appear to reflect on the coupling with the downstream molecule, heterotrimeric G protein. It is likely that the receptors can transduce signals at the pseudopod regions more efficiently than at the tail regions of chemotaxing cells.

What is the role of such kinetic heterogeneity of signaling molecules on signal transduction processes in living cells? In general, modulation of kinetic properties

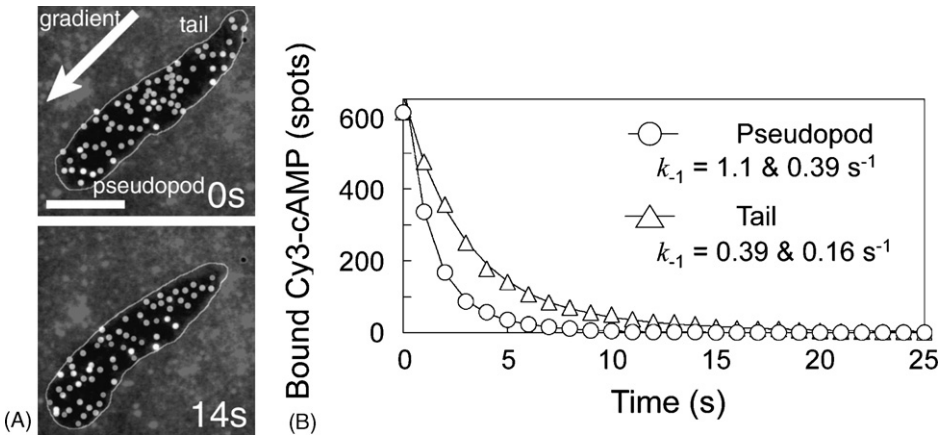

Fig. 10. Heterogeneity of kinetic state in chemotaxis of dictyostelium cells. (A) Image of the binding of fluorescent analogue of cAMP to moving dictyostelium amoeba. (B) The histogram of the duration time of the cAMP binding at the pseudopod and tail halves of the moving cell.

of individual signaling molecules affects not only the average amounts but also the number fluctuations of the ensemble of signaling molecules. This led to a fundamental question on the signaling mechanisms: how can signal quality (S/N ratio) be improved or deteriorated by the stochastic properties of signaling molecules? The answer has been given using theoretical approaches. Shibata and Fujimoto (2005), in which the ratios of signal to noise of the input and output signals are compared when a signaling molecule stochastically generates a second messenger in a Michaelis-Menten type reaction. The average amounts of active signaling molecules (X^*) in a cell are $\overline{X^*}$, which should be accompanied with the noise σ_X. Such noisy signals in the signaling molecule produce noise in the second messengers (Y^*). The average amounts of the second messenger and its noise are expressed as $\overline{X^*}$ and σ_Y, respectively. In the stochastic process, the noise of second messenger concentration can be described by using the *gain–fluctuation relation* (Shibata and Fujimoto, 2005),

$$\frac{\sigma_Y^2}{\overline{Y^*}^2} = g\frac{1}{\overline{Y^*}} + g^2\frac{\tau_X}{\tau_Y + \tau_X}\frac{\sigma_X^2}{\overline{X^*}^2} \tag{1}$$

with

$$g = \frac{\Delta\overline{Y^*}/\overline{Y^*}}{\Delta\overline{X^*}/X^*} = \frac{\partial\ \log\overline{Y^*}}{\partial\ \log\overline{X^*}} \tag{2}$$

where g is the gain of the reaction which is defined as a ratio between the fractional changes in second messenger and active signaling molecules. The τ_X and τ_Y are characteristic time constants of fluctuations in signaling molecules and second messenger concentration, respectively. Because $\sigma_Y/\overline{Y^*}$ and $\sigma_X/\overline{X^*}$ represent the ratio of signal and noise in the outputs and inputs, respectively, Eq. (1) describes the input–output relation in the S/N. Eq. (1) tells us that noise propagation from X^* to Y^* depends on the gain and the characteristic time constants of the corresponding reaction. In chemotactic signaling reactions, the signaling molecule can be referred to as ligand–receptor complex. In this case, the time constant τ_X is defined by $\tau_X = 1/(k_{on}L + k_{off})$, where k_{on} and k_{off} are the association and dissociation rates of ligand, respectively, and L is ligand concentration. Hence, faster dissociation rates of the ligand–receptor complex means a shorter time constant τ_X. With shortening τ_Y, the ratio of the time constants $\tau_Y/(\tau_X + \tau_Y)$ becomes smaller, leading to the decrease of the noise propagation. Therefore, the receptors adopting a faster-dissociation state generate second messengers with higher S/N. Polarity in receptor kinetic states observed in *Dictyostelium* cells implies that the receptors transmit signals with higher S/N at the pseudopod than at the tail regions (Ueda et al., 2001). Thus, kinetic properties of signaling molecules affect the quality of the transmitted signals. Living cells may utilize heterogeneity (or multiple states) of signaling molecules in order to modulate signal quality in stochastic signal processing. Signal and noise propagation along chemotactic signaling system will be discussed in detail elsewhere.

8. Stochastic processes underlying conscious perception

Perception is a processe in which animals recognize stimuli from the outside. In our perception we experience spontaneous alteration between two possible percepts of the figure when we observe an outline of a cube called Necker cube (Fig. 11). The figure can be interpreted in two ways; the upper right square is perceived as the front side of the cube or the lower left square is perceived as the front side of the cube. When we observe it, only one percept out of the two is perceived and the two percepts spontaneously alternate. Another example includes Rubin's vase and faces, Boring's young/old women and bistable apparent motion stimulus. Binocular rivalry in which incongruent images presented to the two eyes competes to be consciously perceived. The subjects were instructed to touch one of two electrodes by

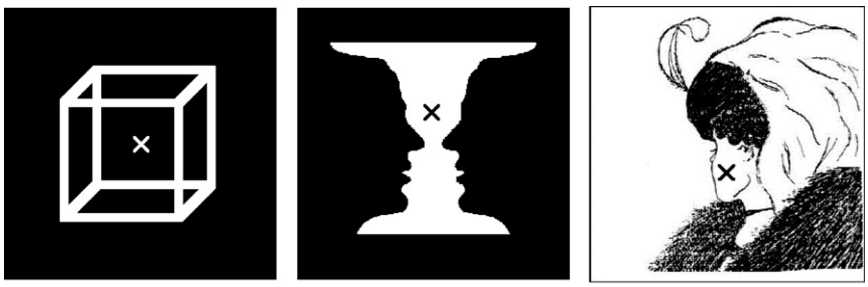

Fig. 11. Figures that can be interpreted in two ways. Necker cube (NC), vase and face (RU) and young and old woman (BO) are depicted.

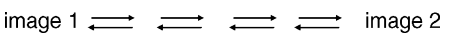

Scheme 6.

their fingers according to their current perception. Their perception was converted to the electric signals and the interval time of the perceptional alteration was analyzed (Murata et al., 2003). The interval time of the perceptional alteration varied and the distribution fit to gamma distribution with natural number α, indicating that the distribution of the interval times of the perceptional alteration is driven from stochastic process in which discrete stochastic events occur with a rate, β, independently of each other and the waiting time, until the αth event occurrence provides the gamma distribution determined by that α (Scheme 6).

9. Conclusions

At various levels of hierarchic structures in biological systems, fluctuation is observed. The perception processes, which are performed in extremely complicated neuron networks in the brain, are described as equations used for molecular dynamics (Murata, private communication). This homology between perception processes and molecular processes leads us to speculate that dynamics at different levels of the hierarchic structures have the same origins. Recently single molecule detection techniques have been developed and allow us to test the idea. The dynamic changes of individual molecules can be measured and are studied in relation to the biological function. Among various proteins and protein assemblies, molecular motors have been most extensively studied. Molecular motors have most fundamental abilities of proteins possessing abilities to catalize the chemical reactions, convert the form of energy, interact with ligands and other proteins and recognize specific molecules. The outcomes of the activities of molecular motors are force and displacement generation. The measurements of such mechanical properties allow them to be measured and analyzed quantitatively and discussed critically.

These results showed that thermal motion is biased in directional motion and reaction through the interaction with other protein molecules. When these molecules self-assemble to higher levels of hierarchic structure of biological systems, unique properties such as cooperativity, memory effects and special asymmetry emerge to make systems function more effectively and flexibly. It is important to understand how these new characteristic features emerge based on stochastic proteins. Single molecule detection techniques have been applied to living cells. In addition to the experimental approaches, the information from the theoretical approaches is helpful.

Biomolecules self-assemble into hierarchic structures and the function is self-controlled. In such systems it is advantageous that various states preexist before stimulation (Kirshner et al., 2000).

References

Arai, Y., Iwane, A.H., Wazawa, T., Yokota, H., Ishii, Y., Kataoka, T., Yanagida, T., 2006. Dynamic polymorphism of Ras observed by single nikecyke FRET is the basis for molecular recognition. Biochem. Biophys. Res. Commun. 343, 809–815.

Finer, J.T., Simmons, R.M., Spudich, J.A., 1994. Single myosin molecule mechanics: piconewton forces and nanometre steps. Nature 368, 113–119.

Funatsu, T., Harada, Y., Tokunaga, M., Saito, K., Yanagida, T., 1995. Imaging of single fluorescent molecules and individual ATP turnovers by single myosin molecules in aqueous solution. Nature 374, 555–559.

Hibino, T., Watanabe, M., Kozuka, J., Iwane, A.H., Okada, T., Kataoka, T., Yanagida, T., Sako, Y., 2003. Single and multiple-molecule dynamics of the signaling from H-Ras to c-Raf-a visualized on the plasma membane of living cells. Chem. Phys. Chem. 4, 748–753.

Ishii, Y., Ishijima, A., Yanagida:, T., 2001. Single molecule nanomanipulation of biomolecules. Trends Biotechnol. 19, 211–216.

Ishijima, A., Yanagida, T., 2001. Single molecule nanobioscience. Trends Biochem. Sci. 26, 438–444.

Ishijima, A., Harada, Y., Kojima, H., Funatsu, T., Higuchi, H., Yanagida, T., 1994. Single-molecule analysis of the actomyosin motor using nano-manipulation. Biochem. Biophys. Res. Commun. 199, 1057–1063.

Ito, Y., Yamasaki, K., Iwahara, J., Terada, T., Kamiya, A., Shirouzu, M., Muto, Y., Kawai, G., Yokoyama, S., Laue, E.D., Walchli, M., Shibata, T., Nishimura, S., Miyazawa, T., 1997. Regional polymorphism in the GTP-boundform of the human c-Ha-Ras protein. Biochemistry 36, 9109–9119.

Iwaki, M., Tanaka, H., Iwane, A.H., Katayama, E., Ikebe, M., Yanagida, T., 2006. Cargo binding makes a wild-type single-headed myosin-VI move processively. Biophys. J. 90, 3643–3652.

Kitamura, K., Tokunaga, M., Iwane, A.H., Yanagida, T., 1999. A single myosin head moves along an actin filament with regular steps of 5,3 nanometres. Nature 397, 129–134.

Kozuka, J., Yokota, H., Arai, Y., Ishii, Y., Yanagida, T., 2006. Dynamic polymorphism of single actin molecules in the actin filament. Nat. Chem. Biol. 2, 83–86.

Kirshner, M., Ferhart, J., Mitchison, J.T., 2000. Molecular "vitalism". Cell 100, 79–88.

Lakowicdz, J.R., 1999. Principles of Fluorescence Spectroscopy. Kluwer Academic/Plenum, New York.

Mehta, A.D., Rock, R.S., Rief, M., Spudich, J.M., Mooseker, M.S., Cheney, R.E., 1999. Myosin-V is a processive actin-based motor. Nature 400, 590–593.

Murata, T., Matsui, N., Miyauchi, N., Kakita, S., Yanagida, T., 2003. Discrete stochastic process underlying perceptual rivalry. Neuroreport 14, 1347–1352.

Nishikawa, S., Homma, K., Komori, Y., Iwaki, M., Wazawa, T., Iwane, A.H., Saito, J., Ikebe, R., Katayama, E., Yanagida, T., Ikebe, M.,

2002. Class VI myosin moves processively along actin filaments backward with large steps. Biochem. Biophys. Res. Commun. 290, 311–317.

Nishiyama, M., Higuchi, H., Yanagida, T., 2002. Chemomechanical coupling of the forward and backward steps of single kinesin molecules. Nat. Cell Biol. 4, 790–797.

Rock, R.S., Rice, S.E., Wells, A.L., Purcell, T.J., Spudich, J.A., Sweeney, H.L., 2001. Myosin VI is a processive motor with a large step size. Proc. Natl. Acad. Sci. U.S.A. 98, 13655–13659.

Schliwa, M. (Ed.), 2003. Molecular Motors. Wiley vch.

Shibata, T., Fujimoto, K., 2005. Noisy signal amplification in ultrasensitive signal transduction. Proc. Natl. Acad. Sci. U.S.A. 102, 331–336.

Svoboda, K., Schmidt, C.F., Schnapp, B.J., Block, S.M., 1993. Direct observation of kinesin stepping by optical trapping interferometry. Nature 365, 721–727.

Taniguchi, Y., Nishiyama, M., Ishii, Y., Yanagida, T., 2005. Entropy rectifies the Brownian steps of kinesin. Nat. Chem. Biol. 1, 346–351.

Ueda, M., Sako, Y., Tanaka, T., Devreotes, P., Yanagida, T., 2001. Single-molecule analysis of chemotactic signaling in Dictyostelium cells. Science 294, 864–867.

van Oudenaarden, A., Theriot, J., 1999. Cooperative symmetry-breaking by actin polymerization in a model for cell motility. Nat. Cell Biol. 1, 493–499.

Weiss, S., 1999. Fluorescence spectroscopy of single biomolecules. Science 283, 1676–1683.